Dispersive FDTD characterisation of no phase-delay radio transmission over layered left-handed meta-materials structure

L. Lu, Y. Hao and C.G. Parini

Abstract: At the interface of two materials with different permittivity and permeability, evanescent waves are excited and will constrain perfect imaging using left-handed meta-materials (LHMs). The dispersive finite-difference time-domain method is used to demonstrate that multilayer stacks, which consist of thin alternating layers of conventional materials and LHMs, can guide evanescent waves with very little attenuation at microwave frequencies and over large stack thicknesses. In addition, such layered structures demonstrate zero phase-delay over the stack thickness, a property that may be applied to construct a no phase-delay transmission line for applications such as beam forming networks for antenna arrays.

1 Introduction

Meta-materials in which both the effective permittivity $\varepsilon(\omega)$ and permeability $\mu(\omega)$ are simultaneously negative [1] over a finite frequency range have received much attention in recent years [2–6]. These materials are typically realised as composite structures that can be constructed from an array of SRRs (split ring resonators) interspersed with a 2D array of wires [4]. Such materials exhibit an antiparalleled nature for the wave (k) and Poynting vectors ($\vec{E} \times \vec{H}$), resulting in extraordinary electrodynamic properties that include reverse Doppler shift, Cherenkov radiation and the inverse Snell effect [1].

It has been demonstrated that a LHM focuses light perfectly even when the material is in the form of a parallel-sided slab [1, 5]. This concept was verified by Ziolkowski [6], using a dispersive finite-difference time-domain (FDTD) method [7–11]. Recently Pendry [12] proposed that a thin LHM slab could be used to enhance the amplitude of evanescent waves in near field imaging. This idea was supported by theoretical [13] and dispersive FDTD numerical results [14–16]. The concept was further developed into a multilayer stack which consisted of thin alternating layers of conventional active materials and lossy LHMs, where such a layered structure could transport evanescent waves over a large stack thickness at the frequency of visible light [17]. Further to this idea we demonstrate in this paper that layered LHM structures can be used to guide evanescent waves with very little attenuation over a large stack thickness at microwave frequencies. Using a two-dimensional dispersive FDTD algorithm it is also shown that such a layered structure exhibits zero phase-delay over its thickness. This property could be used to construct a zero phase-delay transmission line for applications such as beam forming networks for antenna arrays.

IEE Proceedings online no. 20040948

doi:10.1049/ip-smt:20040948

Paper first received 10th March 2004 and in revised form 7th July 2004. Originally published online: 8th December 2004

The authors are with the Department of Electronic Engineering, Queen Mary College, University of London, London E1 4NS, UK

2 Dispersive FDTD formulation on LHM

Simultaneous negative values of permittivity and permeability could be realised only when there is frequency dispersion [1]. The LHM is modelled by causal permittivity and permeability suggested in [18] with the frequency-dependent form

$$\varepsilon_{eff}(\omega) = 1 - \frac{\omega_{ep}^2 - \omega_{eo}^2}{\omega^2 - \omega_{eo}^2 + i\nu\omega} \tag{1}$$

$$\mu_{eff}(\omega) = 1 - \frac{\omega_{mp}^2 - \omega_{mo}^2}{\omega^2 - \omega_{mo}^2 + i\nu\omega} \tag{2}$$

where ω_{eo} is the electric resonant frequency and ω_{ep} is the analogue of the electric plasma frequency, ω_{mo} is the magnetic resonant frequency and ω_{mp} is the analogue of magnetic plasma frequency. In both formulas, $i = \sqrt{-1}$, and ν is the damping factor which is related to the geometry and materials composing the artificial medium. Here $\omega = 2\pi c/\lambda$ is the frequency of the incident wave (c denotes the speed of light in a vacuum). In a 2D LHM media, the frequency-domain constitutive relationship $\hat{D} = \varepsilon\hat{E}$ and $\hat{B} = \mu\hat{H}$ in Maxwell's equations must be rewritten as the following:

$$D_z = \varepsilon_0\left(1 - \frac{\omega_{ep}^2 - \omega_{eo}^2}{\omega^2 - \omega_{eo}^2 + i\nu\omega}\right)E_z \tag{3}$$

$$B_x = \mu_0\left(1 - \frac{\omega_{mp}^2 - \omega_{mo}^2}{\omega^2 - \omega_{mo}^2 + i\nu\omega}\right)H_x \tag{4}$$

$$B_y = \mu_0\left(1 - \frac{\omega_{mp}^2 - \omega_{mo}^2}{\omega^2 - \omega_{mo}^2 + i\nu\omega}\right)H_y \tag{5}$$

The time-domain equations are discretised using the second-order central differences on the standard Yee's lattice in the FDTD method. In this paper only TM excitation is used in the simulation, the electric field E_z is located at the cell centre, and the magnetic fields H_x and H_y are placed at edges of the Yee cell. The sample FDTD iteration equation related to (3) is given by

$$\begin{aligned} &E_z^{n+1}(i+1/2, j+1/2) \\ &= \frac{1}{\varepsilon_0(2 - v\Delta t + \omega_{ep}^2 \Delta t^2)} \\ &\quad \times [(2 - v\Delta t + \omega_{eo}^2 \Delta t^2) D_z^{n+1}(i+1/2, j+1/2) \\ &\quad - 4D_z^n(i+1/2, j+1/2) \\ &\quad + (2 + v\Delta t + \omega_{eo}^2 \Delta t^2) D_z^{n-1}(i+1/2, j+1/2) \\ &\quad + 4\varepsilon_0 E_z^n(i+1/2, j+1/2) \\ &\quad - \varepsilon_0(2 + v\Delta t + \omega_{ep}^2 \Delta t^2) E_z^{n-1}(i+1/2, j+1/2)] \end{aligned} \quad (6)$$

The magnetic fields H_x and H_y can be derived similarly.

There are two approaches to excite evanescent waves in the dispersive FDTD algorithm. The first can be realised when a point source is placed very close to the LHM slab [15, 19, 20]. In this case there will still be minor propagating components, so it is necessary to choose the evanescent source plane a small distance away from the point source [20]. The second approach is based on the so-called pure evanescent wave excitation proposed by Kärkkäinen [14]. For simplicity, we consider two-dimensional transverse magnetic (TM) (E_x, H_x, $H_y \neq 0$) fields oscillating at frequency ω in a source plane at $x = x_0$; the electric components are given by a 2D Fourier expansion as following:

$$E_z(x, y, t) = \begin{cases} \exp(ik_y y + i\sqrt{k_y^2 - \varepsilon_j \mu_j \omega^2/c^2}(x - x_0) - i\omega t) & x > x_0 \\ \exp(ik_y y + i\sqrt{k_y^2 - \varepsilon_j \mu_j \omega^2/c^2}(x - x_0) - i\omega t) & x < x_0 \end{cases} \quad (7)$$

$$E_z(x, y, t) = \begin{cases} \exp(ik_y y - \sqrt{k_y^2 - \varepsilon_j \mu_j \omega^2/c^2}(x - x_0) - i\omega t) & x > x_0 \\ \exp(ik_y y + \sqrt{k_y^2 - \varepsilon_j \mu_j \omega^2/c^2}(x - x_0) - i\omega t) & x < x_0 \end{cases} \quad (8)$$

where (7) can be used to denote propagating fields while (8) represents evanescent waves. As a consequence the evanescent waves will propagate along the transverse y-direction by means of exp ($ik_y y$–$i\omega t$) but decay exponentially from the source along the x-direction.

3 Phase compensation through layered LHM structure

Although the thin LHM slab structure presented in [5] can produce a perfect near field image, the perfectness can be easily dissipated by the lossy LHM and hence reduce the near field resolution. In [17, 21] a multilayer stack consisting of thin alternating layers of conventional materials and LHMs is proposed to eliminate such dissipation. Currently, only equally spaced layered LHM structures have been investigated in the invisible light region. In this paper the effects of the spacing of layered LHM on evanescent wave amplification are investigated in the microwave frequency region.

To verify the validity of our FDTD program a stack with alternating positive and negative dielectric layers was designed to enhance evanescent wave transportation at microwave frequencies. Such a layered structure (Fig. 1) is

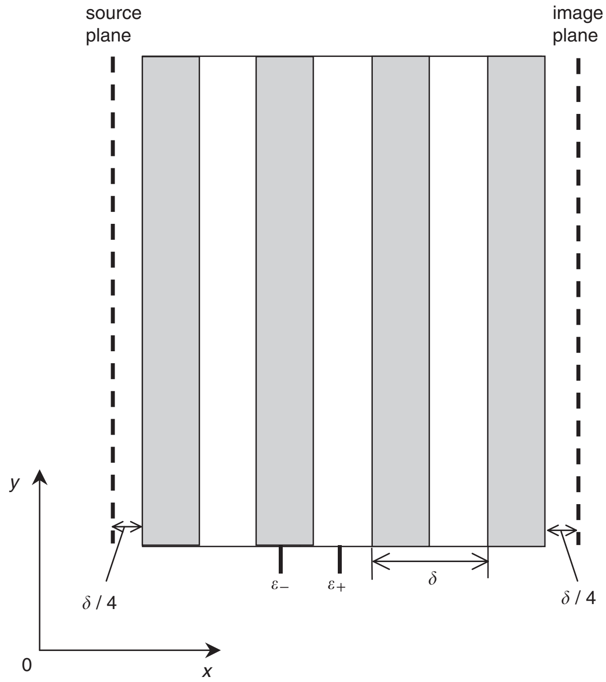

Fig. 1 *Schematic of layered structure*
RHM (positive dielectric) and LHM (negative dielectric) layers have equal thickness as $\delta/2$, total length of multiple layered slabs is $d = [(2N-1\delta)]/2$ where N is number of LHM layers

considered with alternating 'positive dielectrics' with $\varepsilon_{r+} = \mu_{r+} = 1$ and 'negative dielectrics' with $\varepsilon_{r-}(\omega_0) = \mu_{r-}(\omega_0) = -1$ at the target frequency (10 GHz). For the negative dielectrics, $\omega_{pe} = \omega_{pm} = \sqrt{2}\omega_0$, $v = 0$ was used in the FDTD simulation. Currently, a fully stable algorithm of absorbing boundary conditions (ABCs) for LHM is not yet available and hence only conventional ABCs are used in this paper. The proposed multiple-layer structure is located in FDTD space with $\Delta x = \Delta y = \lambda/220$ and surrounded by an eight-cell uniaxial perfectly matched layer (UPML) [22] absorbing boundary. Here a polynomial grading [10] is chosen as the UPML loss profile and the predicted reflection error from the boundary is of order 0.0001. Both the positive and negative dielectric layers are assumed to be of equal thickness $\delta/2$, equivalent to 22 Δx. An evanescent source was excited at a distance of $\delta/4$ (11 Δx) from the multilayer slab. The number N of LHM layers is four, so the total thickness of the layered slabs is $d = (2N-1)\delta/2 = 154\Delta x$. As seen in Fig. 2, unlike

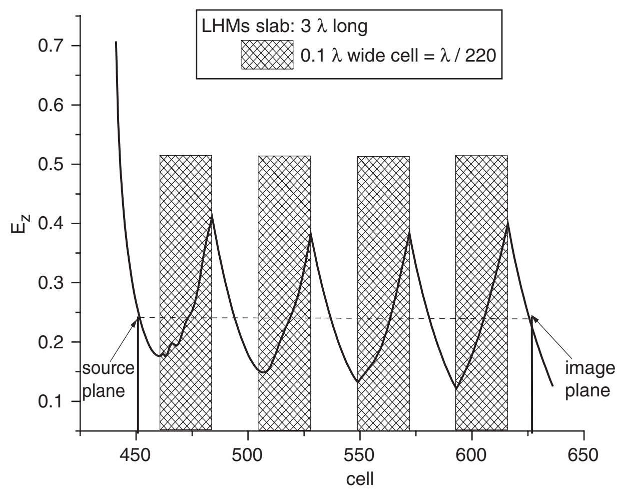

Fig. 2 *Near field intensity through multilayer LHM structure with refractive index n = −1*

conventional evanescent waves that decay exponentially with distance away from the object, the evanescent waves will be enhanced in the LHM slabs due to the excited surface plasmon resonance at the vacuum–LHM slab boundary [3].

Figure 3 demonstrates that when both the positive and negative dielectric layers are assumed to be of equal thickness, as shown in Fig. 1, the layered structure demonstrates no phase-delay over its thickness. The phase velocity expression $v_p = c/n(\omega)$ shows that v_p is related to the index of refraction $n(\omega)$, here c denotes the speed of light in a vacuum. When the LHM's refractive index n is equal to –1, the phase velocity of vacuum v_{pv} will be equal to $-v_{pLHM}$, and consequently the wave will propagate in the backward direction in LHM. Thus the phase of the wave can be kept unchanged after the wave passes through one vacuum slab and one LHM slab that have the same thickness and absolute value of refractive index. This is shown in Fig. 3, where the solid line represents the source and the dashed line represents the electric field on the right boundary of first LHM slab in the layered structure. Accordingly, the other three lines represent the electric field on the right boundary of the second, third and fourth LHM slabs. The numerical result demonstrates that the phases of the electric field at those four locations are identical, indicating that the LHM slab can compensate for the phase-delay of the wave as it goes through one vacuum slab.

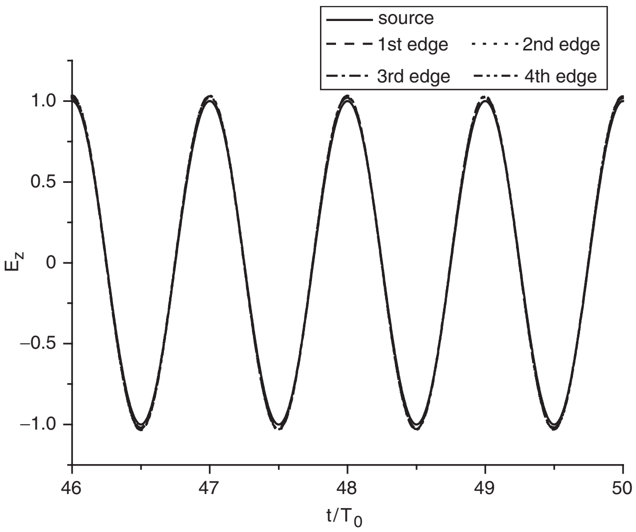

Fig. 3 *Phase compensation for layered structure consisting of alternating layers of vacuum and LHM with refractive index n = −1, thickness of each vacuum and LHM slab being 0.05 λ*

The effects of loss on evanescent wave behaviour is also investigated here, where loss is added to the LHM by choosing the parameters as $\omega_{pe} = \omega_{mp} = \sqrt{2.00005}\omega_0$ and $v = 0.005\omega_0$. In this case, $\varepsilon_r(\omega_0) = \mu_r(\omega_0) = -1 + i\ 0.01$ according to (1) and (2), hence the loss factor is 0.01 and the refractive index of the LHM n is equal to $-1 + i\ 0.01$, with $k_y = \sqrt{2}k_0 = 296.39\ \text{m}^{-1}$. Specifying a large FDTD space of 500 by 500 cells (in terms of 10/10 wavelength), a single LHM slab was placed in the cell region $y = [100, 400]$ and $x = [206, 206 + W]$, with W representing the LHM slab width. Initially, the evanescent wave was amplified with the increase of W, as a consequence of which the image value increased as well, reaching a peak value for W equal to 24 cells (see S(6–24) dashed line in Fig. 4), followed by a gradual suppression of the wave as W was increased from 24 to 60 cells.

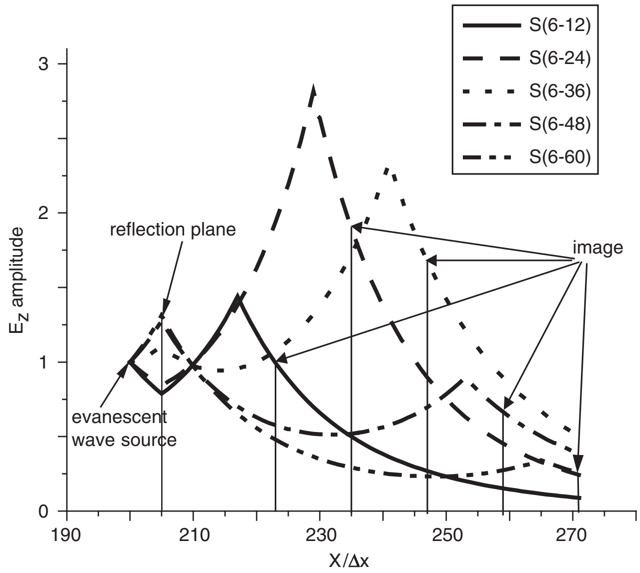

Fig. 4 *Evanescent fields over single LHM slab with different thickness W, W is changed from 12 to 60 cells and distance from source to left surface of LHM slab is 6 cells*

The reasons for amplification are easily explained by the evanescent wave amplification theory caused by the excitation of surface plasmon modes on the vacuum-LHM interface [12]. As for suppression of the wave's peak we believe it is not only caused by the unavoidable lossy absorption [23] but also affected by the increased domination of the left surface (near to the source) plasmon resonance [24] or by surface wave when the LHM slab becomes thicker. It is clearly shown in Fig. 4 that the electric field on the reflected plane (left surface of LHM slab) grows with W. To reduce the dissipation, layered structures with alternating lossy LHM slabs and vacuum slabs with equal and different thickness [17] can be used.

Figure 5 compares the electric field value in these three cases. The distance from the evanescent wave source to the left surface of LHM slab is set as six cells in all cases, and also S (6–84) represents a slab of thickness 84 cells. Similarly, M4 (6–12–12) represents a four-layer structure,

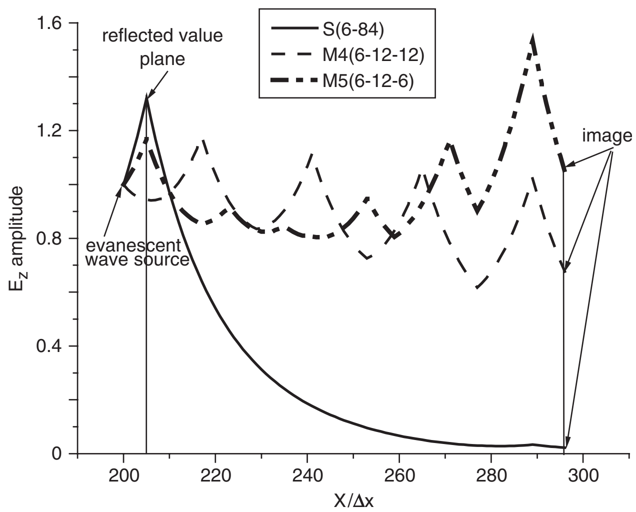

Fig. 5 *Comparison of electric field strengths*
—— single LHM slab
— — multilayer, equal thickness
–--- layered, different thickness

the thickness of each LHM and vacuum slab being 12 cells. Thus the total thickness of layered structure is $(4 \times 2-1) \times 12 = 84$ cells. M5 (6–12–6) represents a five-layer structure, the thickness of LHM slab being 12 cells while the vacuum slab is just six cells, so the total thickness is again $5 \times 12 + (5-1) \times 6 = 84$ cells. The electric field value on the image plane (six cells away from the final right boundary of the LHM slab) is just 0.02 using a single LHM slab. However, this can reach 0.68 using the layered structure with identical thickness and 1.049 with unequal layer thicknesses. Clearly the multilayer LHM structure can amplify the evanescent wave better over a long distance than the single LHM slab, especially when the layered structure employs different slab thicknesses.

4 Conclusions

Evanescent wave behaviour at microwave frequencies in multilayer LHM stacks has been investigated using a dispersive FDTD approach. The layered LHM structure suggested by Pendry can also be used at microwave frequencies to guide the evanescent wave without attenuation over distances and compensate the phase delay resulting from propagation through right-handed materials (RHM).

Loss effects on the evanescent wave behaviour of single and layered LHM slabs have also been demonstrated and such losses can be compensated using layered slabs with reduced gaps to enhance evanescent wave coupling. Future work will include phase compensation for multilayered LHM slabs with different refractive index and thickness.

5 References

1 Veselago, V.G.: ‘The electrodynamics of substances with simultaneously negative values of ε and μ’, *Sov. Phys.-Usp.*, 1968, **10**, (4), pp. 509–514
2 Pendry, J.B., Holden, A.J., Robbins, D.J., and Stewart, W.J.: ‘Magnetism from conductors and enhanced nonlinear phenomena’, *IEEE Trans. Microw. Theory and Tech.*, 1999, **47**, (11), pp. 2075–2084
3 Pendry, J.B.: ‘Negative refraction makes a perfect lens’, *Phys. Rev. Lett.*, 2000, **85**, p. 3966
4 Smith, D.R., Padilla, W.J., Vier, D.C., Nemat-Nasser, S.C., and Schultz, S.: ‘Composite media with simultaneously negative permeability and permittivity’, *Phys. Rev. Lett.*, 2000, **84**, pp. 4184–4187
5 Pendry, J. B.: ‘Focus issue: negative refraction and metamaterials’ Opt. Express, 2003, **11**, (7), p. 639
6 Ziolkowski, R.W., and Heyman, E.: ‘Wave propagation in media having negative permittivity and permeability’, *Phys. Rev. E.*, 2001, **64**, p. 056625
7 Pereda, J.A., Vielva, A., and Prieto, A.: ‘FDTD modeling of wave propagation in dispersive media by using the mobius transformation technique’, *IEEE Trans. Microw. Theory Tech.*, 2002, **50**, (7), pp. 1689–1695
8 Gandhi, O.P., Gao, B.-H., and Chen, J.-Y.: ‘A frequency-dependent finite-difference time-domain formulation for general dispersive media’, *IEEE Trans. Microw. Theory Tech.*, 1993, **41**, pp. 658–665
9 Okoniewski, M., Mrozowski, M., and Stuchly, M.A.: ‘Simple treatment of multiterm dispersion in FDTD’, *IEEE Microw. Guided Wave Lett.*, 1997, **7**, pp. 121–123
10 Taflove, A., and Hagness, S.C.: ‘Computational electrodynamics: the finite-difference time-domain method,’ (Artech House, Norwood, MA, 2000, 2nd Edn.)
11 Yong, J.L., and Nelson, R.O.: ‘A summary and systematic analysis of FDTD algorithms for linearly dispersive media’, *IEEE Antennas Propag. Mag.*, 2001, **43**, (1)
12 Pendry, J.B., and Ramakrishna, S.A.: ‘Imaging the near field’, *J. Phys., Condens. Matter*, 2002, **14**, pp. 8463–8479
13 Gómez-Santos, G.: ‘Universal features of the time evolution of evanescent modes in a left-handed perfect lens’, *Phys. Rev. Lett.*, 2003, **90**, (7), p. 077401
14 Kärkkäinen, M.K., Tretyakov, S.A., Maslovski, S.I., and Belov, P.A.: ‘A numerical study of evanescent fields in backward-wave slabs’, *J. Phys. Condens. Matter.*, 2003, **20**, p. 0302407
15 Cummer, S.A.: ‘Simulated causal subwavelength focusing by a negative refractive index slab’, *Appl. Phys. Lett.*, 2003, **82**, (10), pp. 1503–1505
16 Rao, X.S., Ong, C.K., Rao, X.S., and Ong, C.K.: ‘Amplification of evanescent waves in a lossy left-handed material slab’, *Phys. Rev. B*, 2003, **68**, p. 113103
17 Ramakrishna, S.A., and Pendry, J.B.: ‘Optical gain removes absorption and increases resolution in a near-field lens’, *Phys. Rev. B, Condens. Matter. Phys.*, 2003, **67**, pp. 201101–201104
18 Smith, D.R., and Kroll, N.: ‘Negative refractive index in left-handed materials’, *Phys. Rev. Lett.*, 2000, **85**, pp. 2933–2936
19 Hao, Y., Lu, L., and Parini, C.G.: ‘Time-domain modelling on wave propagation through single/multilayer left-handed meta-materials slab’. Proc. IEE 12th Int. Conf. on Antennas and Propagation (ICAP2003), Exeter, UK, 2003, Vol. 2, pp. 610–613
20 Shen, J.T., and Platzman, P.M.: ‘Near-field imaging with negative dielectric constant lenses’, *Appl. Phys. Lett.*, 2002, **80**, (18), pp. 3286–3288
21 Shamonina, E., Kalinin, V.A., Ringhofer, K.H., and Solymar, L.: ‘Imaging, compression and Poynting vector streamlines for negative permittivity materials’, *Electron. Lett.*, 2001, **37**, (20), pp. 1243–1244
22 Gedney, S.D.: ‘An anisotropic perfectly matched layer-absorbing medium for the truncation of FDTD lattices’, *IEEE Trans. Antennas Propag.*, 1996, **44**, (12), pp. 1630–1639
23 Garcia, N., and Nieto-Vesperinas, M.: ‘Left-handed materials do not make a perfect lens’, *Phys. Rev. Lett.*, 2002, **88**, (20), p. 207403
24 Anantha Ramakrishna, S., Pendry, J.B., Wiltshire, M.C.K., and Stewart, W.J.: ‘Imaging the near field’, *J. Mod. Opt.*, 2003, **50**, pp. 1419–1430